

Solvation Effects on the Stability of Silver(I) Complexes with Pyridine-Containing Ligands Studied by Thermodynamic and DFT Methods

Silvia Del Piero,[†] Rosalisa Fedele,[†] Andrea Melchior,^{*†} Roberto Portanova,[†] Marilena Tolazzi,[†] and Ennio Zangrando[‡]

Dipartimento di Scienze e Tecnologie Chimiche, Università di Udine, Via Cotonificio 108, I-33100 Udine, Italy, and Dipartimento di Scienze Chimiche, Università di Trieste, via L. Giorgieri 1, I-34127 Trieste, Italy

Received January 24, 2007

The formation of Ag(I) complexes with 2,2'-bipyridine (bipy), 2,2'6',2''-terpyridine (terpy), 2-(aminomethyl)pyridine (amp), and bis((2-pyridyl)methyl)amine (dpa) is studied in dimethyl sulfoxide (dmsO) by means of potentiometric and calorimetric measurements. Enthalpy-stabilized mononuclear ML₂ complexes are formed, whereas entropy changes counteract complex formation. Additionally, a comparison with analog Ag–polyamine species is made to evidence the significant different coordination behavior of these classes of ligands. The results are discussed in terms of different basicity and steric requirements of the ligands and solvation effects. The dpa ligand, with an unprecedented coordination pattern, forms also a bimetallic complex [Ag₂(dpa)₂]²⁺ that has been structurally characterized in the solid state by X-ray diffraction. The influence of solvent, water and dmsO, on the binding energy of the monodentate pyridine to Ag(I) has also been assessed by means of density functional theory (DFT) calculations. This study has been extended also in vacuum to the reaction of Ag(I) with the simple monoamine methylamine (mea). These results are correlated with the experimental evidence and used to interpret the different affinities of pyridine for the Ag(I) ion in the two media.

Introduction

The coordination chemistry of silver with nitrogen donors, particularly with polypyridyl ligands, is very rich because of the flexible coordination sphere of this ion and its ability to form, both in solution¹ and in solid state, supramolecular and polynuclear structures with a variety of architectures (3D-networks, chains, sheets).² Furthermore, silver compounds of this class of ligands are able to display interesting features, like supramolecular interactions^{2b} and particular photophysical properties.^{2c}

In recent years, many studies on the thermodynamics of complexation of Ag(I) ion in nonaqueous solvents have been

carried out with a variety of ligands, such as polyamines,^{3,4} amino–phosphines,⁵ aza-macrocycles, cryptands,⁶ and crown ethers¹ to assess the influence of their electronic and steric properties on the stability of the species formed. These studies are also of interest for the practical utility of Ag⁺ as competitive ion in potentiometric studies of complexation of other metals of environmental and technological interest like Pb²⁺, Co²⁺, lanthanides, and alkaline earths.^{3,6b,7}

On the contrary, scarce information is available about the coordination of sp²-hybridized nitrogen donors, such as polypyridines, and the solvent influence on it. This class of ligands has more severe structural constraints and lower

* To whom correspondence should be addressed. E-mail: andrea.melchior@uniud.it. Phone: +39-0432-558882. Fax: +39-0432-558803.

[†] Università di Udine.

[‡] Università di Trieste.

- (1) Thaler, A.; Cox, B. G.; Schneider, H. *Inorg. Chim. Acta* **2003**, *351*, 123.
- (2) (a) Feazell, R. P.; Carson, C. E.; Klausmeyer, K. K. *Inorg. Chem.* **2006**, *45*, 2627. (b) Hanton, L. R.; Young, A. G. *Cryst. Growth Des.* **2006**, *6*, 833. (c) Hou, H.; Wei, Y.; Song, Y.; Mi, M.; Tang, M.; Li, L.; Fan, Y. *Angew. Chem., Int. Ed.* **2005**, *44*, 6067.

(3) Comuzzi, C.; Melchior, A.; Polese, P.; Portanova, R.; Tolazzi, M. *Eur. J. Inorg. Chem.* **2003**, *10*, 1948.

(4) Comuzzi, C.; Novelli, V.; Portanova, R.; Tolazzi, M. *Supramol. Chem.* **2001**, *13*, 455.

(5) Del Zotto, A.; Di Bernardo, P.; Tolazzi, M.; Zanonato, P. L. *J. Chem. Soc., Dalton Trans.* **1999**, *6*, 979.

(6) (a) Abidi, R.; Arnaud-Neu, F.; Drew, M.; Nelson, J. *J. Chem. Soc., Perkin Trans. 2* **1996**, *2*, 2747. (b) Arnaud-Neu, F.; Spiess, B.; Schwing-Weill, M. *J. Am. Chem. Soc.* **1982**, *104*, 5641.

(7) Comuzzi, C.; Di Bernardo, P.; Portanova, R.; Tolazzi, M.; Zanonato, P. L. *Polyhedron* **2002**, *21*, 1385.

σ -donor ability than polyamines, leading to a much weaker affinity for metal ions such as Co^{2+} and Cd^{2+} .⁸ Despite the less negative enthalpic terms of reaction, their different solvation features and lower flexibility with respect to linear polyamines result in a less unfavorable entropic term for the complexation reactions.⁸

In this work, the results concerning the complexation of Ag(I) with the linear polypyridyl ligands 2,2'-bipyridine (bipy) and 2,2',6',2''-terpyridine (terpy), in the aprotic solvent dimethyl sulfoxide (dmsO), are reported and compared with those already given for the simple pyridine (py).^{9a} The mixed ligands, 2-(aminomethyl)pyridine (amp) and bis((2-pyridyl)methyl)amine (dpa), which possess either sp^2 - or sp^3 -hybridized nitrogens, have been also studied to highlight the interplays between steric, electronic, and solvation effects on the nature and stability of the species formed. A comparison is made with results concerning polyamine coordination, as well as with data for the same ligands in aqueous solution. The X-ray single-crystal structure for the $[\text{Ag}_2(\text{dpa})_2](\text{ClO}_4)_2$ dimeric species is also reported.

The influence of the solvation environment, in this case water and the aprotic polar dmsO, on the binding energy of the monodentate pyridine to Ag^+ has been assessed by means of density functional theory (DFT) calculations. Post Hartree–Fock methods have been demonstrated to provide good results in the calculation of structural and spectroscopic properties of silver–pyridine complexes in vacuum^{10,11} and in the calculation of gas-phase binding energies.¹² The hydration of Ag(I) was treated by means of a semicontinuum approach¹³ or explicitly by introducing water molecules in QM/MM MD simulations.¹⁴ In our approach, the solvent molecules are included in the first coordination shell and the bulk effect as a polarized continuum. DFT calculations have been carried out in vacuum also for the coordination of methylamine (mea), chosen as model monoamine, to compare the effect of different σ -donor groups.

Experimental Section

General Remark. Solvated silver salts, $\text{Ag}(\text{ClO}_4)\cdot\text{dmsO}$, the ligands, and solvents were prepared and purified as previously described.^{7,8} The chemicals were stored under inert atmosphere and protected from light.

Potentiometric Measurements. All potentiometric experiments were carried out in a MB Braun 150 glovebox under a controlled atmosphere containing less than 1 ppm of water and less than 1 ppm of oxygen.

In a typical titration, known volumes of ligand solutions ($50 < C^{\circ}_{\text{L}} < 400 \text{ mmol dm}^{-3}$) were added to 20 mL of Ag^+ solutions ($2 < C^{\circ}_{\text{Ag}} < 20 \text{ mmol dm}^{-3}$) at $298.1 \pm 0.1 \text{ K}$. The equilibrium concentrations of Ag^+ were obtained from the emf data of a galvanic cell similar to that previously reported.⁷ Emf data were ascertained on an Amel 338 pH meter equipped with an ion-selective electrode and a Ag/AgCl electrode as reference. The Nernst response of silver electrodes was checked in the range $10^{-7} < \text{Ag}^+ < 10^{-2} \text{ mmol dm}^{-3}$. Equilibrium was typically reached in 2–4 min. The Hyperquad¹⁵ minimization program was used to calculate stability constants.

Calorimetric Measurements. A Tronac model 87-558 precision calorimeter was employed to measure reaction heats. The calorimeter was checked by titration of tris(hydroxymethyl)aminomethane (tham) with a standard solution of HCl in water. The experimental value of the neutralization heat of tham was $\Delta H^{\circ} = -47.59 \text{ kJ mol}^{-1}$, well within the experimental error of the accepted value of $-47.53 \pm 0.13 \text{ kJ mol}^{-1}$.¹⁶

Calorimetric titrations were performed at $298.00 \pm 0.02 \text{ K}$ by adding known volumes of ligand solutions ($50 < C^{\circ}_{\text{L}} < 400 \text{ mmol dm}^{-3}$) to 20 mL of Ag^+ solutions ($2.00 < C^{\circ}_{\text{Ag}} < 50.0 \text{ mmol dm}^{-3}$).

For each titration run, the experimental values of the total heat produced in the reaction vessel were calculated as a function of the added titrant. These values were corrected only for the dilution heat of the titrant, which was separately determined. The dilution heat of the titrate was found to be negligible in the metal concentration range used.

The quantity Δh_v , total heat/mole of metal ion, was defined and calculated by dividing the net reaction heat by the number of moles of metal ion in the calorimetric vessel. The enthalpy values of the complexation reactions have been calculated by least-squares fitting of the experimental heats by computer treatment with the Hyp ΔH program.¹⁷

Crystallography. Single crystals of $[\text{Ag}_2(\text{dpa})_2](\text{ClO}_4)_2$ were grown by dissolution of stoichiometric amounts of silver perchlorate and dpa in acetonitrile followed by the slow diffusion of 2-propanol. As the crystals were rather sensitive to light, they were kept in dark until the collection of diffraction data. Any attempt with other pyridines produced crystals of poor quality.

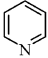
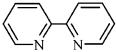
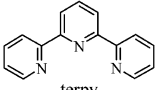
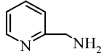
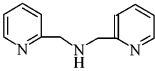
Diffraction data were carried out at 293(2) K on a Nonius DIP-1030H system with Mo $\text{K}\alpha$ radiation ($\lambda = 0.71073 \text{ \AA}$). Cell refinement, indexing, and scaling of the data sets were carried out using Denzo and Scalepack.¹⁸ The structure was solved by Patterson and Fourier analyses and refined by the full-matrix least-squares method based on F^2 with all observed reflections.¹⁹ All the calculations were performed using the WinGX System, ver 1.70.01.²⁰

Crystallographic data: $\text{C}_{24}\text{H}_{26}\text{Ag}_2\text{Cl}_2\text{N}_6\text{O}_8$, $M = 813.15$; monoclinic, space group $C2/c$; $a = 23.768(5)$, $b = 13.363(3)$, $c = 20.343(4) \text{ \AA}$; $\beta = 114.666(10)^\circ$; $V = 5872(2) \text{ \AA}^3$; $Z = 8$; $D_c = 1.840 \text{ g/cm}^3$; $\mu(\text{Mo K}\alpha) = 1.573 \text{ mm}^{-1}$; $F(000) = 3232$; θ range = 1.79 – 26.02° ; final $R_1 = 0.0603$, $wR_2 = 0.1971$, goodness of fit = 0.984 for 380 parameters and 83587 collected reflections; 5711 unique

- (8) Del Piero, S.; Di Bernardo, P.; Fedele, R.; Melchior, A.; Polese, P.; Tolazzi, M. *Eur. J. Inorg. Chem.* **2006**, *18*, 3738.
 (9) (a) Cassol, A.; Di Bernardo, P.; Zanonato, P. L.; Portanova, R.; Tolazzi, M. *J. Chem. Soc., Dalton Trans.* **1987**, *3*, 657. (b) Cassol, A.; Di Bernardo, P.; Zanonato, P. L.; Portanova, R.; Tolazzi, M.; Tomat, G.; Cucinotta, V.; Sciotto, D. *J. Chem. Soc., Faraday Trans. 1* **1989**, *85*, 2445.
 (10) Wu, D. Y.; Ren, B.; Jiang, Y. X.; Xu, X.; Tian, Z. Q. *J. Phys. Chem. A* **2002**, *106*, 9042.
 (11) Pagliai, M.; Bellucci, L.; Muniz-Miranda, M.; Cardini, G.; Schettino, V. *Phys. Chem. Chem. Phys.* **2006**, *8*, 171.
 (12) Wu, Y.; Hayashi, M.; Shiu, Y. J.; Liang, K. K.; Chang, C. H.; Yeh, Y. L.; Lin, S. H. *J. Phys. Chem. A* **2003**, *107*, 9658.
 (13) Martínez, J. M.; Pappalardo, R. R.; Sánchez Marcos, E. *J. Phys. Chem. A* **1997**, *101*, 4444.
 (14) Rode, B. M.; Schwenk, C. F.; Hofer, T. S.; Randolf, B. R. *Coord. Chem. Rev.* **2005**, *249*, 2993.

- (15) Gans, P.; Sabatini, A.; Vacca, A. *Talanta* **1996**, *43*, 1739.
 (16) Martell, A. E.; Smith, R. M.; Motekaitis, R. J. *Critically Selected Stability Constants of Metal Complexes Database*, version 5.0; 1998.
 (17) www.hyperquad.co.uk.
 (18) Otwinowski, Z.; Minor, W. *Processing of X-ray Diffraction Data Collected in Oscillation Mode*. In *Methods in Enzymology Vol. 276*; Carter, C.W., Jr., Sweet, R. M., Eds.; Academic Press: New York, 1997.
 (19) Sheldrick, G. M. *SHELX97 Programs for Crystal Structure Analysis*, release 97-2; University of Göttingen: Göttingen, Germany, 1998.
 (20) Farrugia, L. J. *J. Appl. Crystallogr.* **1999**, *32*, 837.

Table 1. Overall Stability Constants and Thermodynamic Functions for the Reaction $\text{Ag}^+ + j\text{L} \rightleftharpoons \text{AgL}_j^+$ in dmsO at 298 K and $I = 0.1 \text{ mol dm}^{-3}$ (L = Ligand) and in Water

Ligand	Solvent	Species	$\text{Log}\beta_j$	$-\Delta G^\circ_{\beta_j}$ (kJ mol ⁻¹)	$-\Delta H^\circ_{\beta_j}$ (kJ mol ⁻¹)	$-T\Delta S^\circ_{\beta_j}$ (kJ mol ⁻¹)	
 py	dmsO ^a	AgL	1.41	8.05	13.93	5.88	
		AgL ₂	2.11	12.04	40.93	28.9	
	water ^b	AgL	2.00	11.41	20.2	8.79	
		AgL ₂	4.11	23.45	47.4	23.9	
 bipy	dmsO	AgL	2.08(0.01)	11.9(0.1)	20.2(1)	8.3	
		AgL ₂	3.65(0.01)	20.8(0.1)	41.3(1)	20.5	
	water ^c	AgL	3.84	21.9	32.0	10.1	
		AgL ₂	7.37	42.1	49.1	7	
	 terpy	dmsO	AgL	3.03(0.01)	17.3(0.1)	26.6(1)	9.3
			AgL ₂	4.68(0.1)	26.7(0.6)	50(2)	23.3
water ^d		AgL	5.69	-	-	-	
		AgL ₂	9.68	-	-	-	
 amp	dmsO	AgL	3.88(0.01)	22.1(0.1)	33.3(0.5)	11.2	
		AgL ₂	7.63(0.01)	43.5(0.1)	73.5(0.4)	30	
	water ^e	AgL ₃	9.19(0.03)	52.4(0.3)	101(1)	49	
		AgL	4.11	-	-	-	
	 dpa	dmsO	AgL	4.37(0.01)	24.9	37.7(0.3)	12.8
			AgL ₂	7.30(0.01)	41.6	64.2(0.2)	22.6
water ^f		AgL ₂	10.28(0.04)	58.7	93(1)	35.1	
		AgL	5.46	-	-	-	
		AgL ₂	8.16	-	-	-	

^a Reference 9a. ^b Reference 26a. ^c Reference 26b. ^d Reference 26c. ^e Reference 26d. ^f Reference 26e.

[R(int) = 0.0460], of which 3057 with $I > 2\sigma(I)$; maximum positive and negative peaks in ΔF map 1.278, $-0.540 \text{ e \AA}^{-3}$.

Computational Procedure. DFT calculations were performed using the GAMESS-US software²¹ with the B3LYP three-parameter hybrid density functional²² on the ligands and on the following silver complexes: $[\text{Ag}(\text{py})]^+$; $[\text{Ag}(\text{mea})]^+$; $[\text{Ag}(\text{Solv})_3]^+$, $[\text{Ag}(\text{Solv})_4]^+$, $[\text{Ag}(\text{Solv})_3\text{py}]^+$ (Solv = dmsO or H₂O). Note that, in GAMESS-US, the B3LYP functional uses the VWN5 correlation formula.^{22c}

The double split valence Gaussian basis set with added polarization and diffuse functions 6-31++G(d,p) was applied to the atoms of the ligands, and the LANL2DZ ECP²³ was used for the silver ion. All geometries were optimized including symmetry constraints.

After optimization, equilibrium points were characterized by calculating vibrational frequencies, to confirm that they were local minima.

Binding energies were corrected for zero point vibrational energy and thermal energy calculated at 298 K and for the basis set superposition error (BSSE) using the counterpoise correction.²⁴

Solvation effects have been introduced using the PCM model²⁵ with parameters for water and dmsO. For computational convenience, the energies in solution have been obtained by performing a single point energy calculation on the gas-phase optimized structures.

NMR Spectroscopy. ¹H NMR spectra were recorded at 298 K on a Bruker AC-200 spectrometer. Measurements were performed on dmsO-*d*₆ solutions containing AgClO₄ and amp or dpa ligands ($C_L = 57 \text{ mmol dm}^{-3}$) at different molar ratios, $R_c = C_L/C_M$. The spectra are shown in the Supporting Information, Figures S4 and S5.

Results

Solution Thermodynamics. The best-fits of the thermodynamic parameters obtained by the computer treatment of potentiometric and calorimetric data are presented in Table 1. In the same table the stability constants and thermody-

- (21) Schmidt, M. W.; Baldrige, K. K.; Boatz, J. A.; Elbert, S. T.; Gordon, M. S.; Jensen, J. H.; Koseki, S.; Matsunaga, N.; Nguyen, K. A.; Su, S. J.; Windus, T. L.; Dupuis, M.; Montgomery, J. A. *J. Comput. Chem.* **1993**, *14*, 1347.
- (22) (a) Becke, A. D. *J. Chem. Phys.* **1993**, *98*, 1372. (b) Lee, C.; Yang, W.; Parr, R. G. *Phys. Rev. B* **1988**, *37*, 785. (c) Vosko, S. H.; Wilk, L.; Nusair, M. *Can. J. Phys.* **1980**, *58*, 1200.
- (23) Hay, P. J.; Wadt, W. R. *J. Chem. Phys.* **1985**, *82*, 284.

(24) Boys, F. F.; Bernardi, F. *Mol. Phys.* **1970**, *19*, 533.

(25) Tomasi, J.; Mennucci, B.; Cammi, R. *Chem. Rev.* **2005**, *105*, 2999.

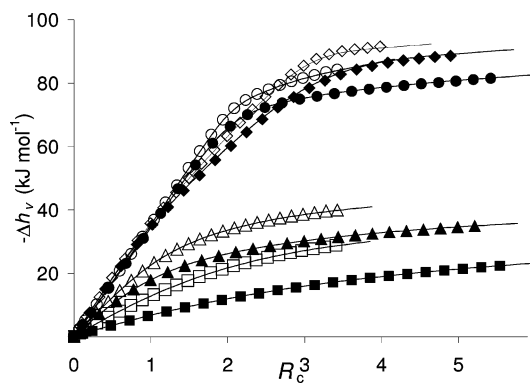


Figure 1. Total molar enthalpy changes ($-\Delta h_v$) as a function of $R_c = C_l/C_M$ for the complex formation in dmso: bipy, (■) 4.9, (□) 20.3 mmol dm^{-3} in Ag^+ ; terpy, (▲) 5.0, (△) 21.1 mmol dm^{-3} in Ag^+ ; amp, (●) 5.0, (○) 19.4 mmol dm^{-3} in Ag^+ ; dpa, (◆) 5.3, (◇) 19.7 mmol dm^{-3} in Ag^+ . Solid lines are calculated from values of β_j and $\Delta H^\circ_{\beta_j}$ in Table 1.

namic functions, previously found in water²⁶ and for $\text{Ag}(\text{I})\text{-py}$ in dmso,⁹ are also listed.

In Figure 1 the total molar enthalpy change (Δh_v), as a function of R_c , is plotted for Ag^+ /ligand systems. The fit between experimental and calculated curves is excellent, and their shapes are fully consistent with information obtained by the analysis of potentiometric data.

The differentiation of the calorimetric curves for the complexation of Ag^+ with bipy and terpy at various C°_{Ag} values is evidence of the formation of complexes of relatively low stability, in agreement with the calculated stability constants for mononuclear AgL^+ and AgL_2^+ species.

In the case of the Ag -aminopyridyl systems, the heats evolved are significantly higher than for Ag -pyridines and the shape of the curves is indicative of the formation of more stable species, at least until $R_c = 1$. At values of $R_c > 1$ the trend agrees with potentiometry results indicating formation of three mononuclear species (Table 1) of decreasing relative stability for amp ($\log K_1 = 3.88$, $\log K_2 = 3.75$, $\log K_3 = 1.56$) and dpa ($\log K_1 = 4.37$, $\log K_2 = 2.93$). Furthermore, potentiometry clearly indicates the formation of the dinuclear species $[\text{Ag}_2(\text{dpa})_2]^{2+}$.

No side reaction, like the ligand oxidation described for $\text{Co}(\text{II})$ -aminopyridyl systems in a previous paper,⁸ has been evidenced here.

Calculated Geometries. The structure of the ligands (dmso and pyridine; see Supporting Information Figures S1 and S2 and Tables S1 and S2) are well described by the method and in excellent agreement with the reported experimental data^{27–29} and with previous quantum mechanical calculations.¹²

The effect of basis set on the calculated structure of dmso was evaluated, evidencing that the use of d-polarization functions produces reliable results also within the Hartree–Fock approximation, while diffuse functions give minor improvements.²⁸

The structures of complexes $[\text{Ag}(\text{Solv})_4]^+$ and $[\text{Ag}(\text{Solv})_3\text{py}]^+$ ($\text{Solv} = \text{dmso}$ or H_2O) and $[\text{Ag}(\text{py})]^+$ optimized in vacuum are shown in Figures 2 and S3 (Supporting Information), and selected bond lengths are reported in Tables 2 and S3 (Supporting Information).

The calculated $\text{Ag}-\text{O}$ distances (Table 2) for $[\text{Ag}(\text{dmso})_4]^+$ (2.412 Å) and $[\text{Ag}(\text{H}_2\text{O})_4]^+$ (2.427 Å) are consistent with recent LAXS and EXAFS results ($\text{Ag}-\text{O}_{\text{dmso}} = 2.39$ Å, $\text{Ag}-\text{O}_{\text{H}_2\text{O}} = 2.43$ Å),³⁰ confirming the reliability of this theoretical approach in predicting also the structural parameters for metal complexes. The structure of the $[\text{Ag}(\text{dmso})_4]^+$ shows a marked distortion with respect to an ideal tetrahedron ($\text{O}-\text{Ag}-\text{O} = 96.9, 96.7,$ and 139.7°) while in $[\text{Ag}(\text{H}_2\text{O})_4]^+$ the $\text{O}-\text{Ag}-\text{O}$ angles are 109.4 and 109.5° .

The $\text{S}-\text{O}$ bond distance in the silver solvate complex of 1.553 Å is longer (+0.03 Å) than that in the free molecule, while the $\text{S}-\text{C}$ bond is shorter (−0.01 Å, Tables 2 and S2, Supporting Information) as usually found for the O-bonded metal complexes.²⁷ The only available crystal structure³¹ of an Ag -dmso solvate, $[\text{Ag}(\text{dmso})_2\text{ClO}_4]_n$, contains infinite chains with dmso molecules bridging the Ag^+ ions, with a weaker $\text{Ag}-\text{O}$ interaction (2.503–2.362 Å) than that found in our calculated structure and in solution studies.³⁰ The $\text{Ag}-\text{N}$ bond distances in $[\text{Ag}(\text{py})]^+$ (Table S3, Supporting Information), $[\text{Ag}(\text{H}_2\text{O})_3\text{py}]^+$, and $[\text{Ag}(\text{dmso})_3\text{py}]^+$ (Table 2) are in excellent agreement with reported data.^{32–34}

The $\text{Ag}-\text{O}$ bonds are slightly modified after pyridine coordination while a significant change in the $\text{O}-\text{Ag}-\text{O}$ angles is observed for both $[\text{Ag}(\text{Solv})_3\text{py}]^+$ complexes (Table 2). The structure of pyridine is unchanged after coordination with a maximum variation of the bond lengths smaller than 0.01 Å (Table 2 and Supporting Information Table S2).

Binding Energies. In Table 3 the reaction enthalpies calculated in vacuum and in the continuum solvation medium are reported. The predicted enthalpy of reaction (-52.3 kJ mol^{-1}) between $[\text{Ag}(\text{H}_2\text{O})_3]^+$ and one water molecule is in satisfactory agreement with the experimental result in gas phase at 298 K ($\Delta H = -62$ kJ mol^{-1}) obtained by high-pressure mass spectrometry.³⁵

The reactions of $[\text{Ag}(\text{H}_2\text{O})_3]^+$ and $[\text{Ag}(\text{dmso})_3]^+$ with one solvent molecule in vacuum display a more favorable ΔH value in the latter case ($\Delta H_{\text{vacuum}} = \Delta H_{\text{vacuum}, [\text{Ag}(\text{H}_2\text{O})_3]^+} - \Delta H_{\text{vacuum}, [\text{Ag}(\text{dmso})_3]^+} = +14.4$ kJ mol^{-1}), while the opposite is found in the solvent medium ($\Delta H_{\text{solv}} = \Delta H_{\text{solv}, [\text{Ag}(\text{H}_2\text{O})_3]^+} - \Delta H_{\text{solv}, [\text{Ag}(\text{dmso})_3]^+} = -13.8$ kJ mol^{-1}). This is mainly due to

(26) (a) Paoletti, P.; Vacca, A.; Arenare, D. *J. Phys. Chem.* **1966**, *70*, 193. (b) Canani, S.; Scrocco, E. *J. Inorg. Nucl. Chem.* **1958**, *8*, 832. (c) Ignaczak, M.; Grzejdzak, A.; Olejniczak, B. *Monatsh. Chem.* **1989**, *120*, 515. (d) Goeminne, A.; Eeckhaut, Z. *J. Inorg. Nucl. Chem.* **1974**, *36*, 357. (e) Anderegg, G. *Helv. Chim. Acta* **1971**, *54*, 509. (f) Anderegg, G.; Hubmann, E.; Podder, N. G.; Wenk, F. *Helv. Chim. Acta* **1977**, *60*, 123.
(27) Calligaris, M. *Coord. Chem. Rev.* **2004**, *248*, 351.
(28) Innes, K. K.; Ross, I. G.; Moomaw, W. R. *J. Mol. Spectrosc.* **1988**, *132*, 492.
(29) Typke, V.; Makkouri, M. *J. Mol. Struct.* **2001**, *599*, 177.

(30) Persson, I.; Nilsson, K. B. *Inorg. Chem.* **2006**, *45*, 7428.
(31) Bjork, N.-O.; Cassel, A. *Acta Chem. Scand. A* **1976**, *30*, 235.
(32) Menchetti, S.; Rossi, G.; Tazzoli, V. *Rend. Ist. Lomb. Acc. Sci. Lett. A* **1970**, *104*, 309.
(33) Nilsson, K.; Oskarsson, A. *Acta Chem. Scand. A* **1982**, *36*, 605.
(34) Wang, Y. H.; Chu, K. L.; Chen, H. C.; Yeh, C. W.; Chan, Z. K.; Suen, M. C.; Chen, J. D.; Wang, J. C. *Cryst. Eng. Commun.* **2006**, *8*, 84.
(35) Holland, P. M.; Castleman, A. W., Jr. *J. Chem. Phys.* **1982**, *76*, 4195.

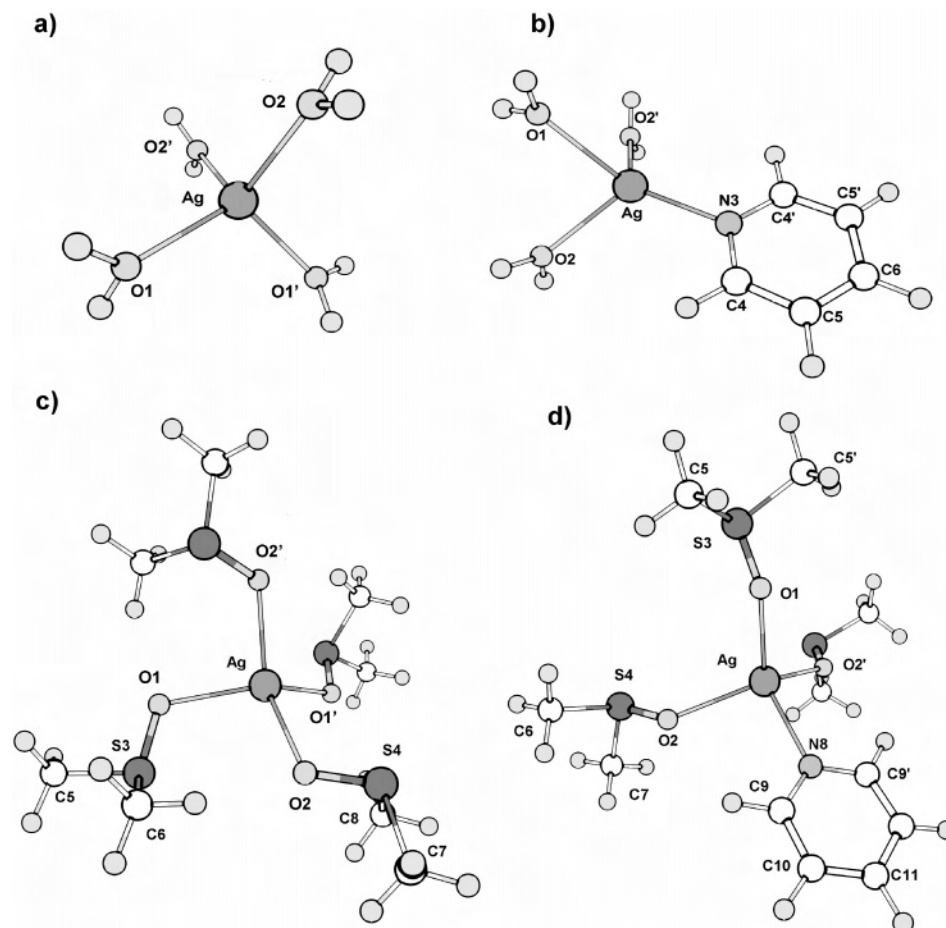


Figure 2. B3LYP-optimized structures of (a) $[\text{Ag}(\text{H}_2\text{O})_4]^+$, (b) $[\text{Ag}(\text{H}_2\text{O})_3\text{py}]^+$, (c) $[\text{Ag}(\text{dmsO})_4]^+$, and (d) $[\text{Ag}(\text{dmsO})_3\text{py}]^+$.

Table 2. Bond Distances and Angles of the Optimized Geometries of Silver–Pyridine Complexes

$[\text{Ag}(\text{H}_2\text{O})_4]^+$				$[\text{Ag}(\text{H}_2\text{O})_3\text{py}]^+$			
bond (Å)		angle (deg)		bond (Å)		angle (deg)	
Ag–O1	2.428	O1–Ag–O2	109.4	Ag–N3	2.244	O1–Ag–O2	83.7
Ag–O2	2.426	O1–Ag–O1'	109.4	Ag–O1	2.418	O2–Ag–O2	99.5
		O1–Ag–O2	109.5	Ag–O2	2.521	O1–Ag–N3	141.1
				C4–N3	1.349	O2–Ag–N3	118.2
				C5–C4	1.393	C4–N3–C4	118.3
				C6–C5	1.396		

$[\text{Ag}(\text{dmsO})_4]^+$				$[\text{Ag}(\text{dmsO})_3\text{py}]^+$			
bond (Å)		angle (deg)		bond (Å)		angle (deg)	
Ag–O1	2.410	O1–Ag–O2	96.9	Ag–N8	2.335	O1–Ag–O2	106.1
Ag–O2	2.413	O1–Ag–O1	139.7	Ag–O1	2.462	O2–Ag–O2	130.2
S3–O1	1.553	O1–Ag–O2	96.7	Ag–O2	2.373	O1–Ag–N8	124.5
S4–O2	1.552	S3–O1–Ag	115.6	S3–O1	1.540	O2–Ag–N8	96.0
S3–C5	1.824	S4–O2–Ag	115.6	S4–O2	1.538	S3–O1–Ag	143.6
S3–C6	1.823			S3–C5	1.827	S4–O2–Ag	134.0
S4–C7	1.824			S4–C6	1.826	C9–N8–C9	118.4
S4–C8	1.824			S4–C7	1.828	C10–C9–N8	122.6
				C9–N8	1.345	C11–C10–C9	118.8
				C10–C9	1.395	C10–C11–C10	118.6
				C11–C10	1.396		

energies (E_{solv}) of the reactants in the two cases: the data reported in Table 4 show that the $[\text{Ag}(\text{Solv})_3]^+$ species is more largely stabilized by solvent with respect to $[\text{Ag}(\text{Solv})_4]^+$ when $\text{Solv} = \text{dmsO}$ ($\Delta E_{\text{solv}} = E_{\text{solv}[\text{Ag}(\text{Solv})_4]^+} - E_{\text{solv}[\text{Ag}(\text{Solv})_3]^+} = +42.3 \text{ kJ mol}^{-1}$) than when $\text{Solv} = \text{H}_2\text{O}$ ($\Delta E_{\text{solv}} = +15.9 \text{ kJ mol}^{-1}$), while the solvation energies of

dmsO and H_2O molecules are quite close ($E_{\text{solv}}^{\text{dmsO}} = -17.2 \text{ kJ mol}^{-1}$ and $E_{\text{solv}}^{\text{water}} = -15.5 \text{ kJ mol}^{-1}$).

The reaction energy in vacuum of the “bare” Ag^+ ion with pyridine is $-203.3 \text{ kJ mol}^{-1}$ (Table 3), compatible with the binding energy previously calculated¹² ($\Delta E = -205.7 \text{ kJ mol}^{-1}$), and overestimates ($\sim +7\%$) the experimental value

Table 3. Reaction Enthalpies (kJ mol⁻¹) Calculated in Different Media at 298 K

reaction	medium		
	vacuum	water	dmsO
Ag ⁺ + py → [Ag(py)] ⁺	-203.3	-93.0	-93.6
Ag ⁺ + CH ₃ NH ₂ → [AgCH ₃ NH ₂] ⁺	-191.1	-105.9	-106.3
[Ag(dmsO) ₃] ⁺ + py → [Ag(dmsO) ₃ py] ⁺	-54.2		-13.0
[Ag(dmsO) ₃] ⁺ + dmsO → [Ag(dmsO) ₄] ⁺	-66.7		-7.2
[Ag(H ₂ O) ₃] ⁺ + py → [Ag(H ₂ O) ₃ py] ⁺	-103.2	-43.7	
[Ag(H ₂ O) ₃] ⁺ + H ₂ O → [Ag(H ₂ O) ₄] ⁺	-52.3	-21.0	

Table 4. Solvation Energies (Vacuum → Solvent) in kJ mol⁻¹ Calculated within the PCM Model

compound	water	dmsO
dmsO		-17.2
H ₂ O	-15.5	
[Ag(dmsO) ₃] ⁺		-118.0
[Ag(dmsO) ₄] ⁺		-75.7
[Ag(H ₂ O) ₃] ⁺	-204.6	
[Ag(H ₂ O) ₄] ⁺	-188.7	

of -189.1 kJ mol⁻¹.³⁶ The results in the two solvents (Table 3) are very close, clearly showing that there is no specific influence of the continuum medium on the reaction enthalpy.

The energy for pyridine binding obtained in vacuum for the aqua complexes is nearly twice than those obtained for the dmsO solvates. The enthalpy values in the solvent are less negative, but, in relative terms, the difference is larger, as we have $\Delta H = -43.7$ kJ mol⁻¹ for the coordination to [Ag(H₂O)₃]⁺ and $\Delta H = -13.0$ kJ mol⁻¹ in the case of [Ag(dmsO)₃]⁺. This trend of the binding energies is in line with the progressive elongation of the calculated Ag-N bond distance (Table 2).

The effect of the electron donation by the coordinated solvent molecules on the acid character of the [Ag(Solv)₃py]⁺ complexes and, therefore, on their affinity for the base can be deduced from the energies of the HOMO of the pyridine and the LUMO of the silver complex, reported in Figure 3.

Also the reaction between Ag⁺ and methylamine (mea) has been studied in vacuum to compare the different behavior of an sp³ N-donor, and the results are given in Table 3. The calculated ΔH in vacuum indicates that mea displays a lower affinity for Ag⁺ than pyridine, while the opposite tendency is observed when the solvent is introduced, indicating a net preference for mea binding both in dmsO and in water (Table 3).

Crystal Structure of [Ag₂(dpa)₂](ClO₄)₂. The crystal consists of dinuclear [Ag₂(dpa)₂]²⁺ complexes and perchlorate anions. An ORTEP view of the former is depicted in Figure 4, and a selection of coordination bond lengths and angles is reported in Table 5. A pair of dpa ligands bridges the two silver ions through the pyridine nitrogen donors to form a helicate structure with metals separated by 2.988(2) Å, typical of Ag-Ag bonds.³⁷ However, the crystal, being centrosymmetric, contains both enantiomers. The complexes are piled along the crystallographic *b*-axis favoring $\pi-\pi$ interactions between py rings of symmetry related complexes. In fact, py rings N(1) and N(6) (at $-x, 2 - y, -z$) and N(3)

and N(4) (at $-x, 1 - y, -z$) show a distance between centroids of 3.770(5) and 3.880(6) Å, respectively, and form a dihedral angle of ca. 20°. The Ag-N_{pyridine} distances fall in a range from 2.159(7) to 2.227(6) Å, but an additional weak interaction is detected between each metal ion and the amine nitrogen of a dpa ligand (mean value 2.435 Å). The conformation of the dpa CH₂NHCH₂ fragment, very similar in the two ligands (mean values for torsion angles of 173.7 and 90.5°), is reached to favor the described long Ag-N interaction and the crystal packing. The Ag-N_{py} bond distances are only slightly longer than those found in the two centrosymmetric dinuclear complexes [Ag₂(amp)₂](ClO₄)₂ (2.146 Å) and [Ag₂(amp)₂](NO₃)₂ (2.175 Å), where the Ag⁺ ions are linearly coordinated by one pyridyl and one aminic nitrogen.³⁸ To our knowledge, the present structure represents an unprecedented coordination behavior for the dpa ligand, and this once more reflects the unusual coordinative behavior of the silver ion. In fact, only mononuclear [M(dpa)₂]ⁿ⁺ complexes have been found with other metals as Ni, Hg, Fe, Cu, Mn, Cd, Zn, Co, and Fe,³⁹ whose octahedral species show M-N_{amine} and M-N_{py} bond lengths of comparable value.

Discussion

Solvent Effect. All complexation reactions are highly exothermic with unfavorable entropic terms (Table 1). The negative enthalpy and entropy values are typical of reactions involving complexation of metal ions by neutral ligands in aprotic solvents.⁴⁰

Pyridine complexes are characterized by higher stabilities in water than in dmsO: the trend is opposite to that found for simple primary and secondary aliphatic amines⁷ where the greater solvation of ligands in water through strong hydrogen bonds⁴¹ overcomes the stronger solvation of metal ions in dmsO.⁴² In this case, the role of ligand solvation is evidently of minor importance and the stability constants follow the trend expected on the basis of the strength of the metal ion solvation. This destabilization of the complex on going from water to dmsO is less marked, as already observed⁸ for Cd²⁺, in the case of amp and dpa. It is evident that the origin of this behavior is the concurrent ligand solvation for the presence of the primary and secondary amino groups. This result confirms that the desolvation of the amino group plays a major role in determining the

(38) Khan, M. A. H.; Prasad, T. K.; Rajasekharan, M. V. *Acta Crystallogr., Sect C: Cryst. Struct. Commun.* **2005**, *61*, m281.

(39) (a) Glerup, J.; Goodson, P. A.; Hodgson, D. J.; Michelsen, K.; Nielsen, K. M.; Weihe, H. *Inorg. Chem.* **1992**, *31*, 4611. (b) Butcher, R. J.; Addison, A. W. *Inorg. Chim. Acta* **1989**, *158*, 211. (c) Davies, C. J.; Solan, G. A.; Fawcett, J. *Polyhedron* **2004**, *23*, 3105. (d) Velusamy, M.; Palaniandavar, M.; Thomas, K. R. J. *Polyhedron* **1998**, *17*, 2179. (e) Huang, G. S.; Lai, J. K.; Ueng, C. H.; Su, C. C. *Transition Met. Chem.* **2000**, *25*, 84. (f) Bebout, D. C.; DeLanoy, A. E.; Ehmman, D. E.; Kastner, M. E.; Parrish, D. A.; Butcher, R. J. *Inorg. Chem.* **1998**, *37*, 2952. (g) Palaniandavar, M.; Butcher, R. J.; Addison, A. W. *Inorg. Chem.* **1996**, *35*, 467. (h) Bebout, D. C.; Stokes, S. W.; Butcher, R. J. *Inorg. Chem.* **1999**, *38*, 1126.

(40) Ahrland, S. *The Chemistry of Non-Aqueous Solvents*; Lagowsky, J. J., Ed.; Academic Press: New York, 1978; Vol. 5a.

(41) Benoit, R. L.; Mackinnon, M. J.; Bergeron, L. *Can. J. Chem.* **1981**, *59*, 1501.

(42) Halidas, A.; Heffer, G.; Marcus, Y. *Chem. Rev.* **2000**, *100*, 819.

(36) Yang, Y. S.; Hsu, W. Y.; Lee, H. F.; Huang, Y. C.; Yeh, C. S.; Hu, C. H. *J. Phys. Chem. A* **1999**, *103*, 11287.

(37) Pykkö, P. *Chem. Rev.* **1997**, *97*, 597.

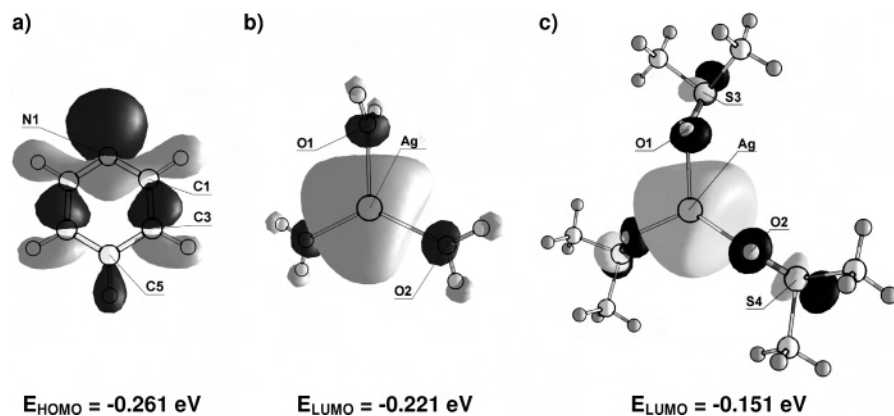


Figure 3. Plots of the HOMO orbital of (a) pyridine and the LUMO of (b) $[\text{Ag}(\text{H}_2\text{O})_3]^+$ and (c) $[\text{Ag}(\text{dmsO})_3]^+$.

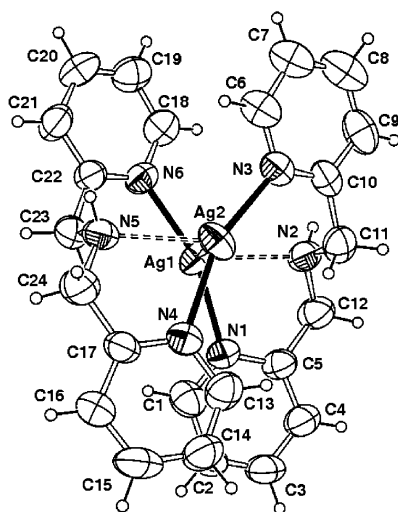
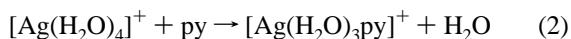
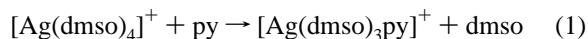


Figure 4. ORTEP drawing (40% probability ellipsoids) of the cation of complex $[\text{Ag}_2\text{dpa}_2](\text{ClO}_4)_2$.

stability trend in the two solvents, while for the pyridyl ligands the metal solvation is more important. This feature has been investigated by means of DFT using a continuum model for outer-sphere solvation effects.

The overall reaction enthalpy of pyridine binding (ΔH_{vacuum} , ΔH_{solv}) can be calculated for the reactions 1 and 2 by combining the reactions in Table 3:



For reaction (1), $\Delta H_{\text{vacuum}} = +12.6 \text{ kJ mol}^{-1}$ and $\Delta H_{\text{solv}} = -5.9 \text{ kJ mol}^{-1}$, and for (2), $\Delta H_{\text{vacuum}} = -50.9 \text{ kJ mol}^{-1}$ and $\Delta H_{\text{solv}} = -22.7 \text{ kJ mol}^{-1}$. These values correctly predict that the overall substitution reactions in the solvent medium are exothermic. The ΔH_{solv} of $-22.7 \text{ kJ mol}^{-1}$ in water is in surprising good agreement with the $\Delta H_{\text{exp}}^\circ = -20.2 \text{ kJ mol}^{-1}$ though no specific interactions (hydrogen bonding) are taken into account in this simple model and the energies in solution have been calculated with the “frozen” geometries optimized in vacuum. The $\Delta H_{\text{solv}} = -5.9 \text{ kJ mol}^{-1}$ for the reaction in dmsO is still close in absolute value to the experimental ($\Delta H_{\text{exp}}^\circ = -13.9 \text{ kJ mol}^{-1}$), even if in relative terms is off by a factor of ~ 2.3 . This deviation may be due to the

approximation mentioned above and in part to the fact that this system is more complex from a quantum mechanical point of view and a higher level of theory would be required to obtain more accurate energies. These results clearly point out that the affinity of pyridine for silver in solution is mainly governed by the bonded solvent molecules in $[\text{Ag}(\text{Solv})_3]^+$ which influence the Ag–pyridine bond formation. The different behavior is essentially due to the degree of electron donation from the coordinated solvent molecules, affecting the energy of the LUMO of silver complex. The energy values found for the HOMO of pyridine ($E = -0.261 \text{ eV}$) and the LUMO of $[\text{Ag}(\text{H}_2\text{O})_3]^+$ ($E = -0.221 \text{ eV}$) and $[\text{Ag}(\text{dmsO})_3]^+$ ($E = -0.151 \text{ eV}$) (Figure 3) show that in the latter case there is a larger electron donation toward the metal producing a stronger destabilization of the LUMO and consequently a worse interaction with the HOMO of pyridine. This is also evidenced by the calculated Mulliken charges (Table S5, Supporting Information) on the metal, equal to $+0.710$ for $[\text{Ag}(\text{H}_2\text{O})_3]^+$ and $+0.572$ for $[\text{Ag}(\text{dmsO})_3]^+$. The intrinsic higher strength of the Ag–pyridine interaction in $[\text{Ag}(\text{H}_2\text{O})_3\text{py}]^+$ is reflected by the significantly shorter Ag–N distance (difference 0.09 \AA ; see Table 2).

The energy spent for the dissociation of one solvent molecule is of minor relevance as the binding energies relative to the reactions $\text{Ag}(\text{Solv})_3^+ + \text{Solv} \rightarrow \text{Ag}(\text{Solv})_4^+$ are quite close in vacuum and even more exothermic as far as water is concerned. If only this reaction was considered, a more favorable interaction of pyridine with the aqua complex would be predicted in gas phase and with the dmsO complex in the solvent.

Pyridyl Ligands. The thermodynamic data for the first complexation step of bipy and terpy ligands in dmsO, compared with those reported for py, are indicative of the formation of bi- and tri-chelated species. The values of $\Delta H_{K_1}^\circ$, lower than what expected if compared with the one of the monodentate py, are associated with the rigidity of the bi- and tridentate ligands, which are not able to reach an optimal binding with all N atoms. The $\Delta H_{K_2}^\circ$ values for the stepwise formation of the $[\text{AgL}_2]^+$ species suggest the formation of a chelated tetrahedral species in the case of bipy whereas, when terpy is concerned, the data seem to fit well the formation of a five-coordinated complex, containing

Table 5. Selected Bonds Distances and Angles of [Ag₂dpa₂](ClO₄)₂

bond (Å)		angle (deg)		torsion angle (deg)	
Ag(1)–N(1)	2.227(6)	N(1)–Ag(1)–N(2)	75.1(2)	C(12)–N(2)–C(11)–C(10)	173.4(6)
Ag(1)–N(2)	2.435(7)	N(1)–Ag(1)–N(6)	159.9(3)	C(11)–N(2)–C(12)–C(5)	87.1(10)
Ag(1)–N(6)	2.169(6)	N(2)–Ag(1)–N(6)	124.1(3)	C(24)–N(5)–C(23)–C(22)	174.1(7)
Ag(2)–N(3)	2.159(7)	N(3)–Ag(2)–N(4)	159.2(3)	C(23)–N(5)–C(24)–C(17)	93.9(11)
Ag(2)–N(4)	2.214(6)	N(3)–Ag(2)–N(5)	125.9(3)		
Ag(2)–N(5)	2.436(7)	N(4)–Ag(2)–N(5)	74.2(2)		

one free pyridine group. This geometry is in accord with several solid-state structures of Ag–terpy compounds.⁴³

Pyridine forms less stable complexes with Ag⁺ ion with less exothermic reactions with respect to monoamines (log $K_{1,n\text{-butylamine}} = 3.58$, $\Delta H^\circ_1 = -31.4$ kJ mol⁻¹).⁴ This result mainly reflects the much lower σ -donor power of pyridine, compared with a primary monoamine, due to hydrogen bonds with the solvent. The ability to form H-bonds has already been invoked when interpreting the gas-phase and solution basicity of primary and tertiary amines.⁴⁴

The introduction of bulk outer-sphere solvation in the energy calculation by DFT is shown to be determinant in explaining the relative affinity of Ag⁺ for pyridine and methylamine. In fact, no significant difference is evidenced from the calculated enthalpy in water and dmsO for both ligands: while the interaction in vacuum is weaker in the case of Ag–mea ($\Delta H = \Delta H_{\text{py}} - \Delta H_{\text{mea}} = -12.2$ kJ mol⁻¹), the opposite trend is found in the two solvents ($\Delta H = \Delta H_{\text{py}} - \Delta H_{\text{mea}} = +12.9$ kJ mol⁻¹ in water and +12.7 kJ mol⁻¹ in dmsO), evidencing the strong bulk effect of the medium. It is interesting to note that a similar result on bulk solvation effects was obtained when comparing the effect of methylation on the coordination of cyclic polyamines on Ni²⁺ and Cr³⁺ in vacuum and in water.⁴⁵

If the thermodynamic parameters for the first step of complexation are compared to those of linear amines with the same number of donor atoms (*n*-butylamine (*n*-but), ethylenediamine (en) and diethylenetriamine (dien))^{4,7} it can be easily observed that $\Delta \log \beta_1$ and the enthalpy gain for pyridines decreases more markedly with the increasing number of N donors. In fact, the $\Delta \log \beta_1$ values ($\Delta \log \beta_1 = \log \beta_{1,\text{pyridine}} - \log \beta_{1,\text{amine}}$) are equal to -2.58 , -3.26 , and -6.47 log units and the ΔH°_1 values ($\Delta H^\circ_1 = \Delta H^\circ_{1,\text{pyridine}} - \Delta H^\circ_{1,\text{amine}}$) are equal to $+17.5$, $+42.8$, and $+51.5$ kJ mol⁻¹, respectively for the mono-, bi-, and tridentate ligands (Table S4, Supporting Information). This effect can be ascribed to the additional structural rigidity of the ligands which limits the possibility of an optimal arrangement around the metal ion and to the higher energy required for the reorientation of the donor groups.

The negative entropy values are due to the loss of translational and conformational degrees of freedom of the ligands, which are not compensated by the increase of disorder due to the release of dmsO molecules from the metal.

For pyridines the reaction entropy is systematically less unfavorable than for the polyamines of same hapticity ($T\Delta S^\circ_1 = -32.5$ and -35.6 kJ mol⁻¹ for en and dien, respectively, Table S4). This result is only in part related to the lower conformational freedom of polypyridines. A second important factor, which can be invoked to explain such negative entropy for polyamines, is the increase of local order around the complex through hydrogen bonds with surrounding solvent molecules: the results reported in this work are an indirect proof of this effect, since the formation of hydrogen bonds for pyridines is not possible and therefore the associated negative entropic contribution is missing.

Amino–Pyridyl Ligands. The amino–pyridyl ligands display an intermediate behavior between those of polyamines and polypyridines. In fact, the thermodynamic parameters of Table 1 origin from the balance of the electronic and solvation effects of the two functionalities, and from a structural point of view, are closer to those of polyamines for their relatively high flexibility.

A comparative analysis of the thermodynamic data obtained for mono- and poly-dentate aliphatic amines^{4,7,9} and for pyridines is not so unambiguous in indicating the involvement also of pyridyl nitrogens in metal complex formation, especially when amp is involved. The thermodynamic data for the first step of complexation by the monodentate *n*-butylamine formation are, in fact, very near to those found for amp. Nevertheless, the ¹H NMR spectrum of amp in presence of Ag⁺ at $R_c = 0.8$ (Figure S4, Supporting Information) is proof of the chelating behavior of the ligand. There is a significant modification of the chemical shift of the aromatic protons with respect to the free ligand; in particular, the multiplet centered at 7.20 ppm is rather sensitive to coordination of Ag⁺ and shifted by 0.23 ppm (7.43 ppm) indicating the coordination of the pyridine moiety.

In the case of dpa, the ¹H NMR spectra at $R_c \leq 1$ (Figure S5, Supporting Information) show that the singlet at 3.83 ppm in the free ligand (–CH₂– protons) is shifted by 0.14 ppm (3.97 ppm) after complexation and the broad signal due to the proton of the secondary amino group is shifted by 1.5 ppm on complex formation (from 2.98 to 4.48 ppm). The shift of the aromatic protons (in the range 7–9 ppm) after complexation confirms also in this case the binding of the pyridine unit. The coordination of the aminic groups is evident also at higher molar ratio ($R_c \geq 1.5$), along with the minor change of chemical shift of pyridine protons with respect to free dpa which suggests the opening of (at least) one pyridine in [Ag(dpa)₂]⁺. This observation is in agreement with the values of the thermodynamic parameters.

The bidentate behavior of amp is also effective in the second complexation step, as suggested by the relative high

(43) (a) Fu, Y.; Sun, J.; Li, Q.; Chen, Y.; Dai, W.; Wang, D.; Mak, T. C. W.; Tang, W.; Hu, H. *J. Chem. Soc., Dalton Trans.* **1996**, *11*, 2309.

(b) Hannon, M. J.; Painting, C. L.; Plummer, E. A.; Childs, L. J.; Alcock, N. W. *Chem.–Eur. J.* **2002**, *8*, 2225.

(44) Meyerstein, D. *Coord. Chem. Rev.* **1999**, *185*, 141.

(45) Clark, T.; Hennemann, M.; van Eldik, R.; Meyerstein, D. *Inorg. Chem.* **2002**, *41*, 2927.

value of the stability constants ($\log K_2 = 3.75$). The associated high negative $\Delta H^\circ_{K_2}$ value (-40 kJ mol^{-1}), even more exothermic than $\Delta H^\circ_{K_1}$, is in line with a greater solvation present in the first complexation step, as confirmed also by the entropic term. The weak stability of the third complex certainly results from the opening of at least one pyridinic Ag–N bonds due to the coordination of the third amp ligand.

In addition to the mononuclear species, dpa forms dinuclear complexes in dmsO even if in lower extent: this does not occur in water, despite the difference in the dielectric constants of the two solvents (78.5 for water and 46.4 for dmsO), which should induce stronger electrostatic repulsion between metal ions in dmsO than in water. Evidently, the higher stability of the $[\text{AgL}]^+$ species in water than in dmsO prevents the formation of the dimeric $[\text{Ag}_2\text{L}_2]^{2+}$. The existence of this bimetallic species of Ag(I) ion in dmsO solution is supported by its isolation also in the solid state. In dmsO solution the same interactions observed in the solid state are likely to be present and the Ag–Ag bond interaction should be suggested. This hypothesis is in line with the high negative enthalpy and entropy terms associated with $[\text{Ag}_2\text{-dpa}_2]^{2+}$ when compared to those relative to $[\text{Agdpa}]^+$.

Conclusions

The comparative study of Ag^+ –pyridines interaction in dmsO and water demonstrates that the different solvation of the metal ion determines the stability of the complexes formed, in an opposite way than what was found for polyamines. The results on silver complexation with polypyridines are useful also in the interpretation of the whole coordination thermodynamics of polyamines in dmsO, confirming that the formation of H-bonds by the coordinated ligand is a fundamental contribution to the high negative entropy in the latter case. The amino–pyridines have an

intermediate thermodynamic behavior between the two classes of ligands, and in the case of dpa, they are able to form bimetallic species both in solution and in solid state.

The DFT calculations well predict the structures of the complexes and reproduce the trends of reaction energies between Ag^+ and pyridine in water and dmsO. The results point out that the affinity of pyridine for silver in solution is governed by the stabilizing effect of the first-shell solvent molecules in $[\text{Ag}(\text{Solv})_3]^+$ on the Ag–N bond formation, through the different degrees of electron donation in the case of water and dmsO. On the other hand, the energy paid for the dissociation of one solvent molecule from $[\text{Ag}(\text{Solv})_4]^+$ in the two media is of minor importance.

Finally, the reaction with methylamine, considered as a model molecule for primary amines, is strongly influenced by the presence of continuum solvation showing that, in addition to the formation of H-bonds, the bulk effect plays an important role in influencing the relative affinity toward silver.

Acknowledgment. Special thanks go to Pierluigi Polese (University of Udine) for his technical support.

Supporting Information Available: X-ray crystallographic data in CIF format, Figures S1–S3 and Tables S1–S3, containing the optimized geometries and structural parameters of dmsO, pyridine, and $[\text{Agpy}]^+$ complex, Table S4, containing literature data on Ag–polyamine complexation in dmsO, Table S5, collecting the calculated Mulliken charges on the silver complexes, and Figures S4 and S5, showing the ^1H NMR spectra for the Ag–amp and –dpa systems in dmsO- d_6 . This material is available free of charge via the Internet at <http://pubs.acs.org>.

IC070124D